3D Analysis of Transmural Myocardial Strain from Sonomicrometric Crystals in the Open Chest Dog

G Saracino[1,2], A Ragnoni[1,2], Z Popovic[1], C Corsi[2], N Greenberg[1],
C Lamberti[2], JD Thomas[1]

[1]Cleveland Clinic, OH, USA
[2]Bologna University, Bologna, Italy

Abstract

Interest in left ventricular (LV) mechanics has recently focused on detailed 3D analysis of LV deformations. Our goal is to investigate transmural strain variability within the normal ventricle and during the early stages of ischemia using sonomicrometric crystals implanted into canine LV wall. In this study 3 open chest dog models were implanted in a two-tetrahedron configuration with three crystals on the epicardial surface, three on the endocardial surface and one in the LV midwall. Our algorithm numerically reconstructs local ventricular 3D geometry and mechanics including radial, longitudinal and circumferential strain. Along with EKG, pressure-volume signals were acquired using a catheter introduced to LV from the femoral artery.

Results obtained clearly illustrate a difference in strain across the myocardium. This study shows that the method can disclose important information regarding transmural variability in animal model and further investigation with different pacing and conditions could enhance understating of LV Mechanics.

1.   Introduction

Interest in left ventricular (LV) mechanics has recently focused on detailed 3D analysis of LV deformations [1-8]. Early stages of ischemia and necrosis always affect the inner layer of myocardial tissue first [4,8]and the role of detailed transmural analysis is not only important for improved understanding of LV mechanics[9-15] but above all for prospects of early detection, treatment and monitoring of such conditions.

In this study, our goal is to develop a method for the analysis transmural strain variability within left ventricular wall using sonomicrometic crystals and then apply our methodology to investigate strain variability within the normal ventricle and during the early stages of ischemia and necrosis.

2.   Methods

We have developed a method of implanting of up to 16 sonomicrometric crystals into LV wall in order to measure regional deformations in open chest dog model. Sonomicrometric crystals emit and receive ultrasonic pulses that can be used to assess the relative distance between transmitter and receivers. In this study, 3 open chest dog models were implanted in a two-tetrahedron configuration with three crystals on the epicardial surface, three on the endocardial surface and one in the LV midwall. Additional crystals were implanted in the LV apex, at the origin of LAD coronary artery, and to the anchoring point of the midline of the posterior mitral valve leaflet in order to impose a fiducial plane.

Our algorithm numerically reconstructs the relative position in 3D space of sonomicrometric crystals that were implanted in animal hearts throughout the cardiac cycle. The initial set of x,y,z coordinates of each crystal is iteratively adjusted to minimize an error function that weights the matrix of transmitter-receiver distances with a computed quality factor of each signal acquired. The reconstructed 3D configuration of the crystals and its deformation during the cardiac cycles is then used to provide information regarding the local ventricular 3D geometry and mechanics including radial, longitudinal and circumferential strain. The EKG signal was acquired and used to separate each cardiac cycle and correlate results from different cycles and animal models. Pressure-volume signals were also acquired using a catheter introduced to LV from the femoral artery.

2.1.   Reconstruction of geometry

Let $\bar{x}_i = (x_i, y_i, z_i)$ and $\bar{x}_j = (x_j, y_j, z_j)$ be the reconstructed position in the 3D coordinates system of two crystals and d_{ij} the measured distance from the i-th to the j-th crystal, we can define the *signed squared error* term e_{ij} as :

$$e_{ij} = (x_i - x_j)^2 + (y_i - y_j)^2 + (z_i - z_j)^2 - d_{ij}^2$$

The 3D geometry of the implanted crystals can be reconstructed by minimizing the following error function F:

$$F = \alpha \sum_{i=1}^{N} \sum_{j=1}^{N} \theta_{ij} e_{ij}^2$$

where θ_{ij} is an element of the constant matrix θ, which characterizes the "quality" of the signals obtained with the i-th crystal as a transmitter the j-th as a receiver; α is a factor used to normalize the error function and it is defined as:

$$\alpha = \sum_{i=1}^{N} \sum_{j=1}^{N} 1 \Big/ \sum_{i=1}^{N} \sum_{j=1}^{N} \theta_{ij}$$

In our implementation we iteratively adjust the current solution by an increment h in the direction of the descendent gradient using the method of Levenbergh-Marquardt which calculates h solving the following system:

$$(G(x) + uI)h = -g(x);$$

where G is the second derivative of the function to be minimized, g is the first derivative and u is a positive number large enough to guarantee that $(G(x) + uI)$ is defined positive.

The first derivative of the error function, for the k-th crystal position is:

$$g_k = dF / d\bar{x}_k = \alpha \sum_i \sum_j \theta_{ij} \frac{d(e_{ij}^2)}{d\bar{x}_k}$$

$$= \alpha \sum_i \left(\theta_{i,k} \frac{d(e_{i,k}^2)}{d\bar{x}_k} \right) + \sum_j \left(\theta_{k,j} \frac{d(e_{k,j}^2)}{d\bar{x}_k} \right)$$

$$= \alpha \sum_j 4(\bar{x}_k - \bar{x}_j)(\theta_{k,j} e_{k,j} + \theta_{j,k} e_{j,k})$$

The second derivative in respect to the k-th and l-th crystals can be derived as follows:

$$G_{k,l} = d^2 F / d\bar{x}_k d\bar{x}_l = \frac{d}{d\bar{x}_l} \frac{dF}{d\bar{x}_k}$$

$$= \alpha \sum_j \frac{d}{d\bar{x}_l} \left[4(\bar{x}_k - \bar{x}_j)(\theta_{k,j} e_{k,j} + \theta_{j,k} e_{j,k}) \right]$$
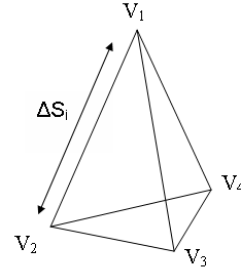
For $k \neq l$, it becomes:

$$d^2 F / d\bar{x}_k d\bar{x}_l = \alpha \frac{d}{d\bar{x}_l} \left[4(\bar{x}_k - \bar{x}_l)(\theta_{k,l} e_{k,l} + \theta_{l,k} e_{l,k}) \right]$$

$$= \alpha \{ -4(\theta_{k,l} e_{k,l} + \theta_{l,k} e_{l,k}) - 8(\bar{x}_k - \bar{x}_l)^2 (\theta_{k,l} + \theta_{l,k}) \};$$

Instead, for $k=1$:

$$d^2 F / d\bar{x}_k d\bar{x}_l = d^2 F / d\bar{x}_k d\bar{x}_k$$

$$= \alpha \sum_j \left[(\theta_{k,j} e_{k,j} + \theta_{j,k} e_{j,k}) + (\bar{x}_k - \bar{x}_j)(\theta_{k,j} \frac{de_{k,j}}{d\bar{x}_k} + \theta_{j,k} \frac{de_{j,k}}{d\bar{x}_k}) \right]$$

$$= 4\alpha \sum_j \left[(\theta_{k,j} e_{k,j} + \theta_{j,k} e_{j,k}) + 2(\theta_{k,j} + \theta_{j,k})(\bar{x}_k - \bar{x}_j)^2 \right]$$

2.2. Strain analysis

In a given x,y,z coordinate system, the relationship between the LaGrangian strain tensor E, the projections the i-th side of the tetrahedron $(\Delta a_1, \Delta a_2, \Delta a_3)_i$ onto the three orthogonal axes and the length of the i-th side between two time points is represented in the following equality:

$$(\Delta S - \Delta S_0)_i = 2[\Delta a_1 \quad \Delta a_2 \quad \Delta a_3]_i \begin{bmatrix} E_{11} & E_{12} & E_{13} \\ E_{21} & E_{22} & E_{23} \\ E_{31} & E_{32} & E_{33} \end{bmatrix} \begin{bmatrix} \Delta a_1 \\ \Delta a_2 \\ \Delta a_3 \end{bmatrix}_i$$

If we consider $\begin{cases} E_{21} = E_{12} \\ E_{31} = E_{13} \\ E_{32} = E_{23} \end{cases}$, we obtain from the above:

$$(\Delta S - \Delta S_0)_i = 2(E_{11} \Delta a_1^2 + E_{22} \Delta a_2^2 + E_{33} \Delta a_3^2 + 2E_{12} \Delta a_1 \Delta a_2 + 2E_{13} \Delta a_1 \Delta a_3 + 2E_{23} \Delta a_2 \Delta a_3)_i$$

For each i = 1,…,6 as the tetrahedron sides.

In our implementation, once we reconstruct the geometry of the sonomicrometric crystals for each time frame we choose a reference system and solved the following system of i equations to obtain E:

$$\begin{bmatrix} \Delta S_1^2 - \Delta S_{01}^2 \\ .... \\ .... \\ \Delta S_6^2 - \Delta S_{06}^2 \end{bmatrix} = \begin{bmatrix} (2\Delta a_1^2 & 4\Delta a_1 \Delta a_2 & 4\Delta a_1 \Delta a_3 & 2\Delta a_2^2 & 4\Delta a_2 \Delta a_3 & 2\Delta a_3^2)_1 \\ & ..... & ..... & & & \\ & ..... & ..... & & & \\ & ..... & ..... & & & \\ & ...... & ..... & & & \\ (...... & ...... & ...... & .... & ...... & ....)_6 \end{bmatrix} \begin{bmatrix} E_{11} \\ E_{12} \\ E_{13} \\ E_{22} \\ E_{23} \\ E_{33} \end{bmatrix}$$

It can be re-written in compact form as: $\Delta S = XE$ and solved by inverting the matrix X: $E = X^{-1}\Delta S$

3.   Results

The acquisition of clean signals from the crystals posed a great challenge in this study. Acquisitions were full of noise due to interference, mechanical movements of the crystals and bleeding in proximity of the implantation area.

The algorithm was able to successfully reconstruct the 3D geometrical shape of the implanted crystals, although in some instances we had to fine tune the matrix of the weight factors.

Results obtained clearly illustrate a difference across the myocardium in terms of magnitude, direction and timing of the mechanical contraction.

During the cardiac cycle the endocardial areas decreased in the time between QRS and T (Fig.1) with an extent of the contraction which was proportional to the size of the heart. In the same time frame, the epicardial areas first showed a slight increase immediately after QRS, then decreased with velocities which were different in each model. The recovery phase of both endocardial and epicardial areas were characterized by an oscillating pattern.

epicardial strain.   Regional strain in the radial, longitudinal and circumferential directions were considerably different in the pericardial and endocardial regions (Fig.2).

4.   Discussion and conclusions

This study shows that the method used can disclose important information regarding transmural variability in an animal model. Our study shows considerable transmural variability of LV strain in an open-heart animal model. Thus, using a single descriptor of deformation, as often used in clinical assessment of strain, may be very misleading. Further investigations under varying experimental conditions, such as modulation of ventricular activation or ischemia, could further enhance our understanding of LV mechanics and its applicability in the clinical arena.
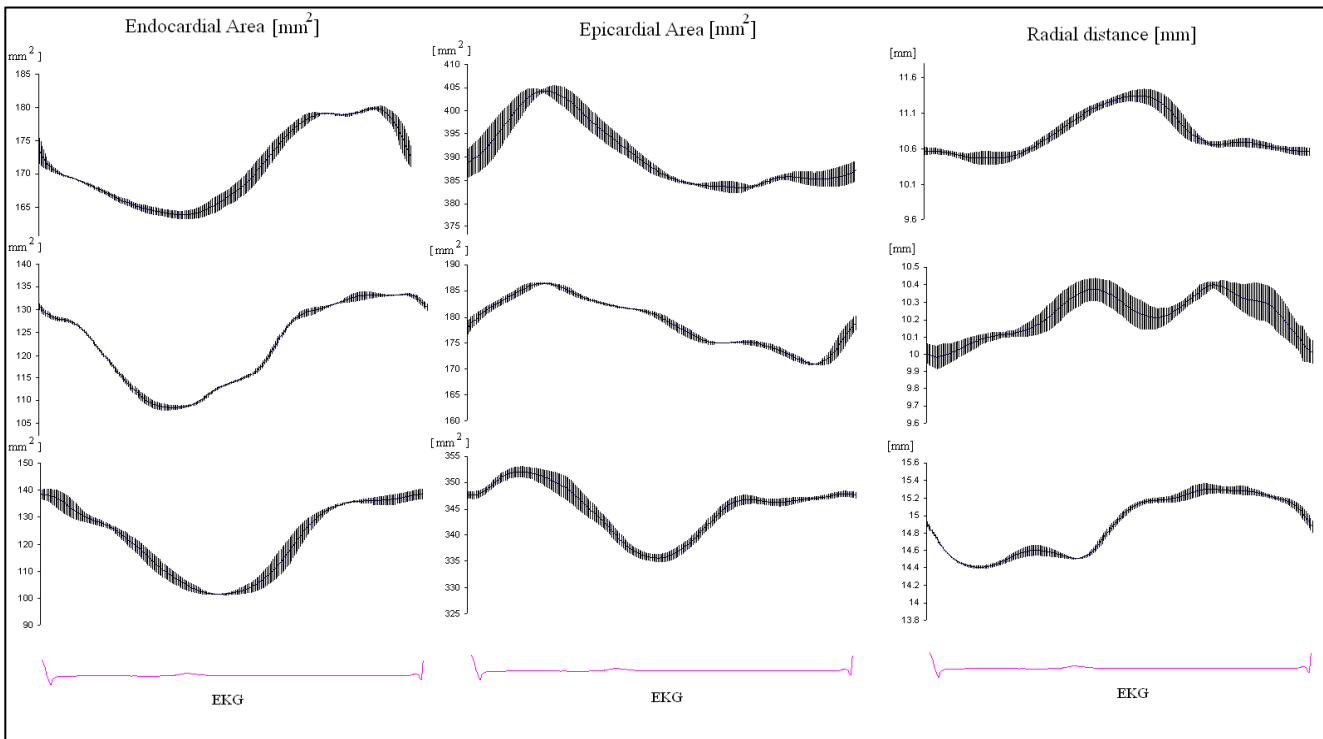
Acknowledgements

Figure 1. From left to right, the endocardial, epicardial surface areas and the distances in the radial direction of the tetrahedronal bases (Average ± SD) obtained in 10 consecutive beats from the reconstructed geometry of the crystals implanted in a double tetrahedron configuration.
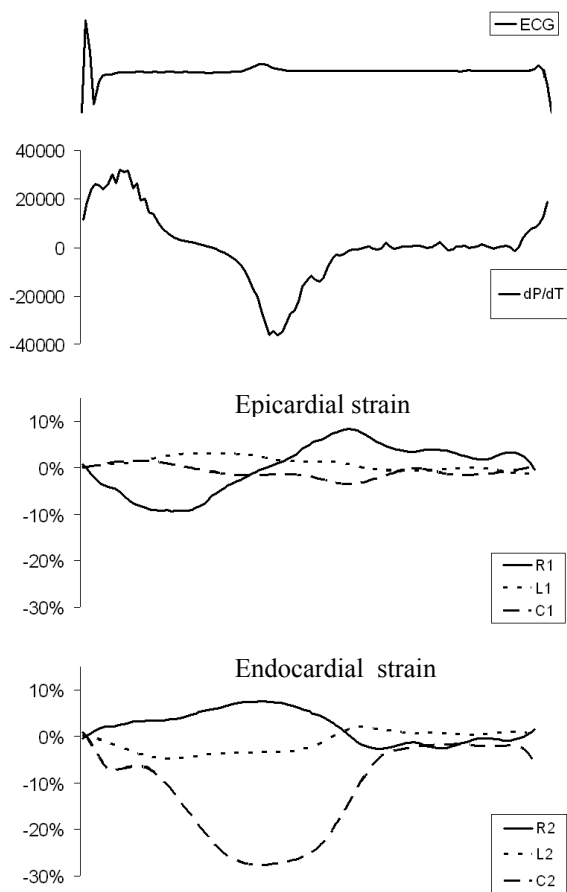
Figure 2. Radial, longitudinal and circumferential strain obtained from the endocardial tetrahedron, on the lower part, and the epicardial tetrahedron, second from bottom

References

[1] Kowalski M, Kukulski T, Jamal F, Dhooge J, Weidemann F, Rademakers F. Can natural strain and strain rate quantify regional myocardial deformation? A study in healthy subjects. Ultrasound Med Biol 2001;27:1087-1097.

[2] Hatle L, Sutherland GR. Regional myocardial function a new approach. Eur Heart J 2000;21:1337-1357.

[3] Waldman LK, Fung YC, Covell JW. Transmural myocardial deformation in the canine left ventricle normal in vivo three-dimensional finite strains. Circ Res 1985;57:152-163.

[4] Prinzen FW, Arts T, Van der Vusse G, Reneman RS. Fiber shortening in the inner layers of the left ventricular wall as assessed from epicardial deformation during normoxia and ischemia. J Biomech 1984;17:801-811.

[5] Prinzen FW, Augustijn CH, Arts T, Allessie MA, Reneman RS. Redistribution of myocardial fiber strain and blood flow by asynchronous activation. Am J Physiol 1990;259:300-308.

[6] Freeman GL, LeWinter MM, Engler RL, Covell JW. Relationship between myocardial fiber direction and segment shortening in the midwall of the canine left ventricle. Circ Res 1985;56: 31–39.

[7] Hiroshi A, Criscione JC, Omens JH, Covell JW, Ingels NB. Transmural left ventricular mechanics underlying torsional recoil during relaxation. Am J Physiol Heart Circ Physiol 2004;286: 640-647.

[8] Arai AE, Gaither CC, Epstein FH, Balaban RS, Wolff SD. Myocardial Velocity Gradient by Phase Contrast MRI with application to regional function in myocardial ischemia. Magn Reson Med 1999;42:98-109.

[9] Jamal F, Bergerot C, Argaud L, Loufonat J, Ovize M. Longitudinal strain quantifies regional right ventricular contractile function. AJP Heart 2003;285:2842-2847.

[10] Sengupta PP, Khanderia BK, Korinek J, Wang J, Belohlavek M. Biphasic tissue Doppler waveforms during isovolumic phases are associated with asynchronous deformation of subendocardial and subepicardial layers. Journal of Applied Physiology 2005;99:1104-1111.

[11] Tibayan FA, Lai DTM, Timek TA, Dagum P, Liang D, Daughters GT, Ingels NB, Miller DC. Alterations in left ventricular torsion in tachycardia-induced dilated cardiomyopathy. J Thorac Cardiovasc Surg 2002;124:43-9.

[12] Urheim S, Edvarsen T, Torp H, Angelsen B, Smiseth OA. Myocardial Strain by Doppler Echocardiography – validation of a new method to quantify regional myocardial function. Circulation 2000;102:1158-1164.

[13] Dione DP, Shi P, Smith W, DeMan P, Soares J, Duncan J, Sinusas A, Three-dimensional regional left ventricular deformazion from digital sonomicrometry, In Proceedings of the 19th Engineering in Medicine and Biology 1997;30:848-851.

[14] Radcliffe MB, Gupta KB, Streicher JT, Savage EB, Bogen DK, Edmunds LH. Use of sonomicrometry and multidimensional scaling to determine the three dimensional coordinates of multiple cardiac locations: feasibility and initial implementation. IEEE Trans Biomed Eng 1995;42:587-598.

[15] Meyer SA, Wolf SA. Application of sonomicrometry and multidimensional scaling to cardiac catheter tracking. IEEE Trans Biomed Eng 1997;44:1061-1067.

Address for correspondence

James D. Thomas , MD
Cardiovascular Medicine, Desk F15
The Cleveland Clinic
9500 Euclid Ave
Cleveland, OH 44195
thomasj@ccf.org